COMMISSION INTERNATIONALE
DES GRANDS BARRAGES

VINGT-CINQUIÈME CONGRÈS
DES GRANDS BARRAGES
Stavanger, Juin 2015

OPTIMIZING THE SUSTAINABILITY OF SEDIMENT BYPASS TUNNELS TO COUNTER RESERVOIR SEDIMENTATION (*)

Christian AUEL
Senior Researcher, Dr. Sc. ETH, Disaster Prevention Research Institute, Kyoto University, formerly, Laboratory of Hydraulics, Hydrology and Glaciology (VAW), ETH Zurich

Michelle HAGMANN
PhD Student, M. Sc. ETH

Ismail ALBAYRAK
Senior Researcher, Dr. Sc. EPFL

Robert M. BOES
Director, Prof. Dr. sc. techn. ETH

Laboratory of Hydraulics, Hydrology and Glaciology (VAW), ETH Zurich

SWITZERLAND

1. INTRODUCTION

Sediment bypass tunnels (SBT) route sediment load around man-made reservoirs avoiding accumulation in the water body. They are an effective countermeasure against reservoir sedimentation and therefore contribute to a sustainable use of storage capacity for water supply, flood control and hydropower. Most tunnels are located in alpine regions at small to medium-size reservoirs where a considerable amount of coarse material is entrained. Japan and Switzerland are among the leading countries in the number of operated tunnels. Due to the fact that sedimentation affects reservoirs worldwide, bypass tunnels recently gain

(*) *Optimisation de la durée de vie des galeries de dérivation de sédiments pour contrer la sédimentation des réservoirs.*

interest in other mountainous regions in Asia such as Taiwan and Nepal or in South America such as Ecuador and hence knowledge on SBT construction, operation and maintenance becomes more and more important.

Sediment bypass tunnels are operated at supercritical open channel flow conditions to ensure sufficient transport capacity and to keep the cross sectional area small and thus construction costs low. Challenging difficulties arise due to high flow velocities and as a result high of sediment flux. As a consequence all worldwide existing bypass tunnels are exposed to severe hydroabrasion damages on the tunnel invert. As a striking example the Palagnedra SBT in the canton of Ticino, Switzerland is shown in Fig. 1, where a vast flood event occurred in 1978 causing an about 2 m deep incision channel destroying the invert on the entire tunnel length and endangering the tunnel foundation [1, 2].

Fig. 1
Invert damages in Palagnedra SBT, canton of Ticino, Switzerland. Horseshoe tunnel cross section with about 2 m deep abrasion channel.
Dégâts sur le radier de la galerie de dérivation de sédiments de Palagnedra, dans le canton du Tessin, Suisse. Une partie de la galerie présente un canal d'abrasion de 2 m de profondeur.

These hydroabrasion damages cause high annual maintenance costs up to about 1% of the overall construction expenses inhibiting the construction of future sediment bypass tunnels [2]. To decrease these costs the tunnel design and the invert materials have to be improved. Therefore the Laboratory of Hydraulics, Hydrology and Glaciology (VAW) of ETH Zurich initiated two research projects to address these issues [2, 3, 4]. The main goal is to establish general design criteria for optimum hydraulic conditions to avoid sediment depositions in the tunnel and to keep the invert abrasion damages at a minimum.

In order to develop these design criteria a sound understanding of the fundamental physical processes present in sediment bypass tunnels is essential. In the first project the mean and turbulent flow characteristics of supercritical open channel flow, the particle motion on fixed beds, and the abrasion development in space and time caused by transported sediment were investigated by means of a hydraulic model in the laboratory [2]. The second project deals with various invert materials, their durability and economy. By conducting *in-situ* experiments, the abrasion resistance of different materials under real operating conditions has been investigated and compared with the life cycle cost. Herein, the results and design recommendations derived from both studies are presented.

2. LABORATORY RESEARCH STUDY

In the laboratory research investigation, new insights were gained on the dynamics of small- and large-scale turbulence structures, particle motion, resulting bed abrasion and their interactions in a supercritical open channel flow over a fixed bed, where the roughness height k_s is some orders of magnitude smaller than the transported particle diameter D ($k_s << D$). The project was divided into three main test series according to the main objectives of the study:

Phase A: Mean and turbulent flow characteristics
Phase B: Particle motion
Phase C: Invert abrasion caused by sediment transport

All experiments were conducted in a $b = 0.30$ m wide, 0.7 m high and 13.50 m long glass- and PVC-sided tilting flume (Fig. 2). The flume slope was adjustable from $S_b = 0.01$ to 0.04. At the flume end the water dropped from 1.50 m into a pool and was recirculated in an enclosed system with a maximum discharge of $Q = 250$ l/s. The discharge was transferred from pressurized to supercritical free-surface flow using a jetbox developed at VAW [5]. The model scale factor was $\lambda_s \approx 15$ compared to typical dimensions of existing bypass tunnels in Japan and Switzerland.

Fig. 2
Hydraulic model flume in the VAW laboratory.
Modèle hydraulique à l'échelle réduite dans le laboratoire de VAW.

The standard flume bed was concrete-lined with an abrasion resistant mortar layer. This invert was used for test phase A and B. For test phase C, the downstream part of the model invert material was replaced by a weak mortar mixture to allow for abrasion. Downscaling of the invert was challenging for both the transported sediment and the invert. Whereas sediments could be geometrically downscaled, a substitute material had to be found for the tunnel invert. Similarities were found from bedrock erosion research where concrete-like materials were applied in scaled hydraulic models to simulate bedrock [6, 7, 8]. Two different weak mortar mixtures were prepared to simulate the abrasion process in the model flume. The mixtures consisted of uniform fine sand (D = 1-1.4 mm) as aggregate, water and Portland cement CEM 1 42.5N. The water/cement (*wc*) ratio was kept constant with a value of 0.6, the aggregate/cement (*ac*) ratio was chosen very low with 10 and 15, termed *hard* and *soft mixture*, respectively. The mortar blocks were produced in advance outside of the flume by the in-house workshop to allow for both constant construction procedure and adequate curing time. To ensure reasonably homogeneous blocks each mortar was mixed in a rotary-drum mixer. Compaction was done by hand in a prefabricated formwork due to its dry conditions similar to a tamped concrete.

2.1. EXPERIMENTAL RESULTS

In phase A, 9 test runs were conducted using a two dimensional - Laser Doppler Anemometry (2D-LDA) system to measure the instantaneous streamwise and vertical velocities [2, 9]. From the obtained data, turbulence intensities, friction velocities, bed and Reynolds shear stresses were calculated. The results showed that the mean and turbulence flow characteristics appear to be universal and hence are well presented with the majority of existing equations in literature. Minor deviations from universality were only observed to some extent when strong secondary currents are present, i.e. in narrow open channel flows (with b = flume width, and h = flow depth $b/h < 4$). These secondary current cells redistributed the turbulence intensities and bed shear stress across the flume leading to 20-50% higher shear stress values close to the side walls compared to the average. The secondary currents became weaker toward the flume center and almost disappeared at higher aspect ratios, i.e. for wide open channel flow ($b/h > 5$), and a more randomly distributed bed shear stress pattern was observed.

In phase B, 5,280 single particle motions were recorded using a high-speed camera to determine their transport mode, particle velocities, saltation trajectories, and impact energies on the bed [2, 10]. The results showed that particles were dominantly transported in saltation mode with minor parts in rolling mode and some small particles in suspension. The particle saltation probability was found to be as a function of the Shields parameter independent of particle size and shape. The particle velocity scaled linearly with the flow velocity, showing excellent correlation and negligible effect of particle size and shape. The saltation trajectory was described by the hop height and length of a particle. The hop height and length linearly correlated with the Shields parameter. Both parameters were highly sensitive to the Shields number and slightly sensitive to the bed slope, whereas an effect of particle shape was negligible.

The specific particle impact energy was calculated using the impact velocity before particle bed collision, the amount of impacts and the particles transported in time. The number of impacts was expressed as a function of hop length and transport mode probability. The obtained specific energy increased with the Shields parameter towards a certain maximum and decreased beyond due to two opposite effects. Whereas the single impact energy per particle increased with increasing flow intensity, the number of impacts showed an opposite trend. At a certain flow condition these two effects canceled each other. Furthermore it was shown that the energy due to sliding and rolling motion was constant being independent of particle size and flow velocity. Further analysis showed that in the streamwise direction particles were 3% slower after bed collision, whereas in the vertical direction they were on average 40% higher after impact. This is associated with the effect of a lift force due to vertical directed turbulence structures in the inner wall region.

In phase C, the abrasion development in space and time was investigated [2]. The results showed that bed abrasion mostly initiated downstream of a bed irregularity and progressed in time both in the lateral and vertical direction. The abrasion mainly developed at two lateral incision channels along the flume side walls, some runs showed randomly distributed potholes, and others showed a mixture of both. Lateral channels were always observed at low aspect ratios b/h < 3-4, whereas the latter were observed at higher aspect ratios b/h > 3-4. The lateral incision channels matched well with the spanwise bed shear stress distribution across the flume. At locations of high bed shear stress high bed abrasion was observed. In return, these lateral channels stabilized the bottom vortices, i.e. secondary currents, thus revealing a self-intensifying process. At higher aspect ratios the more randomly distributed bed shear stress caused a more randomly distributed abrasion pattern.

Abrasion continuously increased with time revealing a balanced state where the amount of transported sediment and abraded mortar linearly scaled. Examining the abrasion rate in detail separately for every varied parameter revealed that abrasion (I) increased with flow intensity and sediment transport rate, (II) showed the highest values for the mean particle diameter category, and (III) decreased with increasing material strength. In contrast to bedrock river studies [6, 7, 8], the flow was always supercritical and no abrasion-damping cover effect was observed. However, for the small particles a damping effect was observed where abrasion was considerably lower compared to other experiments due to both inter-particle contacts and low individual particle mass and thus kinetic energy.

2.2. ABRASION PREDICTION MODEL

Sklar and Dietrich [11] formulated a widely applied *saltation-abrasion model* to predict the abrasion rate of bedrock rivers depending on the particle saltation trajectory, particle velocity and bedrock properties:

$$A_r = \frac{Y_M}{k_v f_t^2} W_{im}^2 \cdot \frac{1}{L_p} \cdot q_s \left(1 - \frac{q_s}{q_s^*}\right) \qquad \text{[m/s]} \qquad [1]$$

where q_s = effective gravimetric sediment transport rate [kg/(sm)], q_s^* = gravimetric bedload transport capacity [kg/(sm)], W_{im} = mean vertical particle impact velocity [m/s], Y_M = Young's Modulus of elasticity [Pa], L_p = particle saltation length [m], k_v = rock resistance coefficient [-], and f_t = rock tensile strength [Pa]. The last term in brackets on the right in Eq. (1) is related to the cover effect occurring at high bedload transport rates partly or totally covering the bed. The impact energy is decreased and thus the bed protected. Eq. (1) is presented in a slightly modified version applied for hydraulic structures prone to supercritical flows using [2, 10]:

$$A_r = \frac{Y_M}{k_v f_t^2} W_{im}^2 \cdot I \cdot q_s \qquad \text{[m/s]} \qquad [2]$$

where I = number of particle impacts per meter. The widely accepted value of k_v is 1.0×10^6 [11, 12]. Based on [12] the coefficient k_v is not only valid for bedrock, but also concrete abrasion. Note that in Eq. (2), f_t denotes the tensile strength of the concrete tunnel invert. The cover effect term in Eq. (1) is dropped due to the fact that Auel [2] did not observe any cover tendencies in supercritical flows. Sklar and Dietrich [11] developed equations for the estimation of W_{im} and L_p in Eq. (1). However, they are not applicable for saltating particles in highly supercritical flows [2, 10]. Therefore, new equations for these terms based on [2, 10, 12] are introduced for Eq. (2).

In the following, the design equations obtained from the experiments are summarized and a computational example based on prototype data of the Solis SBT in Grisons, Switzerland, is given.

To accurately design a SBT, the design discharge Q_d, the cross-sectional dimensions or at least the tunnel width b_t, and the tunnel invert slope S_b have to be defined. Furthermore, knowledge of the river width and slope as well as the mean sediment particle diameter D_m present in the catchment upstream of the considered tunnel intake location is indispensable. Preferably, the particle size distribution should also be known. To accurately describe the resistance of the tunnel invert, the invert material strength and Young's modulus are required.

2.2.1. Hydraulic parameters

As most of the tunnels consist of a steeply sloped acceleration section, followed by a mildly sloped section, the flow is not always uniform along the tunnel length L_t but accelerated at first and decelerated downstream of the break of slope. Thus, the flow depth h has to be calculated using a 1D backwater curve calculation. From the continuity equation the average streamwise flow velocity U_{co} is calculated as

$$U_{co} = \frac{Q_d}{b_t h} \qquad \text{[m/s]} \qquad [3]$$

where Q_d is design discharge. The friction velocity U_* follows as

$$U_* = \sqrt{g R_h S} \qquad \text{[m/s]} \qquad [4]$$

with R_h = hydraulic radius and S = energy line or bed slope. If uniform flow applies, the bed slope S_b can be used instead of the energy line slope S_e. The

friction velocity for a wide river, where $h<<B$, with B = river width may be calculated using the flow depth h instead of R_h. The Shields parameter θ follows as

$$\theta = \frac{U_*^2}{(s-1)gD_m} = \frac{R_h S}{(s-1)D_m} \qquad [-] \qquad [5]$$

where D_m = mean particle diameter and $s = \rho_s/\rho$, with ρ_s = particle density and ρ = water density.

In order to calculate the flow velocity in the upstream river, the Gauckler-Manning-Strickler equation can applied as follows

$$U = \frac{1}{n} R_h^{2/3} S_b^{1/2} \qquad [m/s] \qquad [6]$$

where n = Manning coefficient, and S_b = bed slope. Assuming a wide river where $R_h \approx h$ and applying the continuity equation, Eq. (6) can be rewritten as

$$h = \left(\frac{Q \cdot n}{B\sqrt{S_b}} \right)^{3/5} \qquad [m] \qquad [7]$$

2.2.2. Transport capacity

Bed-load sediment transport in the river system upstream of a reservoir may be calculated using [13] who proposed a revised version of [14] as

$$q_{vn}^* = 4.93\left(\theta - 0.047\right)^{1.6} \qquad [-] \qquad [8]$$

where q^*_{vn} = non-dimensional volumetric bedload transport capacity. The value 0.047 in Eq. (6) equals the critical Shields parameter given by [14] with $\theta_c = 0.047$. Typical θ_c values for movable beds vary from $0.052 < \theta_c < 0.086$ [15]. The non-dimensional volumetric bedload transport capacity follows as

$$q_{vn}^* = \frac{q_v^*}{\sqrt{(s-1)gD^3}} \qquad [-] \qquad [9]$$

with q_v^* as specific volumetric bedload transport capacity per unit width in [m^3/(sm)], and D = characteristic particle diameter. Note that typically $D = D_m$.

In bypass tunnels, the relative roughness is low ($k_s/h << 0.1$, with k_s = equivalent sand roughness height). Thus the bedload transport may be estimated using [2], [16], or [17]. Pedroli [16] proposed for $S_b \leq 0.02$

$$q_s^* = 14.5 \cdot \frac{\tau_b^{8/5} D_m^{1/5} g^{3/5}}{\rho_s^{3/5} \nu^{1/5}} - 23.2 \rho_s \nu \qquad \text{[kg/(sm)]} \qquad [10]$$

where $\tau_b = \rho R_h S$ given in the unit [kg/m^2], g = gravitational acceleration and ν = kinematic viscosity. Note that the difference between q_v^* and the specific gravimetric bedload transport capacity q_s^* is only given by the sediment particle density with $q_s^* = q_v^* \rho_s$. Smart and Jäggi [17] proposed for low relative roughness

$$q_s^* = q \cdot \frac{7.35 \rho_s}{(s-1)} \left(\frac{D_{90}}{D_{30}} \right)^{0.2} S_b^{1.6} \left(1 - \frac{\theta_c}{1.5\theta} \right) \qquad \text{[kg/(sm)]} \qquad [11]$$

where q = specific water discharge [m^3/(sm)], and D_{30} and D_{90} as the characteristic diameters, at which 30 and 90% of a sample's mass are comprised of smaller particles. The choice of the critical Shields parameter θ_c is challenging. For fixed and smooth or transitionally rough bed where $k_s << D$ applies, critical values are one order of magnitude lower compared to alluvial rough river beds due to the fact that the sediment particle is totally exposed to the flow. [18] and [19] proposed $\theta_c = 0.007$, whereas in [2] an average value of $\theta_c = 0.002$ is found. However, the choice of θ_c at highly supercritical flows as present in SBTs is not crucial if $\theta_c < 0.01$ is considered. The last term on the right hand side of Eq. (11) tends to be unity at high flow intensities where θ is high and θ_c is low.

Additionally a formula derived from the data analysis in [2] may be used. Note that this formula is based on only 10 experiments partially conducted at non-uniform flow conditions:

$$q_{vn}^* = 24.0 \left(\theta - \theta_c \right)^{1.5} \qquad \text{[-]} \qquad [12]$$

where $\theta_c = 0.002$ based on hydraulic model test results. The low critical Shields parameter is due to the fact that sediment transport occurs on a fixed bed with $k_s/h << 0.1$.

The bedload transport capacity calculated in the bypass tunnel has to exceed the transport capacity in the upstream river section in order to secure a safe bypassing of all incoming sediment, i.e.

$$Q_{tunnel}^* > Q_{river}^* \qquad \text{[kg/s]} \qquad [13]$$

Eqs. (10), (11) and (12) are proposed for the calculation of bedload transport in the tunnel, whereas Eq. (8) or any other state of the art bedload transport formula as for example from [20] is proposed to calculate the transport in the river system.

2.2.3. *Particle impact velocity*

At saltation motion a particle impinges the bed transferring its kinetic energy. The vertical particle impact velocity W_{im} is crucial to determine the impact energy and can be approximated based on [12] as follows

$$W_{im} = U_* \qquad \text{[m/s]} \qquad [14]$$

2.2.4. *Number of particle impacts*

The number of particle impacts I is required to estimate the impact energy per unit length and is defined as the reciprocal value of the hop length L_p as

$$I = \frac{\left(1-\left(U_*/V_s\right)^2\right)^{0.5}}{L_p}\left(1-P_R\right) \quad 0 \le P_R \le 1 \qquad \text{[1/m]} \qquad [15]$$

where V_S = particle settling velocity and P_R = rolling probability. The numerator of the first term on the right hand side is proposed by [11] and accounts for the mode shift from saltation to suspension. Fits for the rolling probability P_R and the saltation length L_p were found in [2, 10] by data analysis and can be applied in Eq. (15) as follows:

$$I = \left(\frac{\left(1-\left(U_*/V_s\right)^2\right)^{0.5}}{251\theta D}\right)\left[1-8.5\cdot 10^{-4}\left(\theta\left(\frac{k_s}{D}\right)^2\right)^{-0.55}\right] \qquad \text{[1/m]} \qquad [16]$$

Note that Eq. (16) is only valid for a low relative bed roughness with $k_s << h$ and $k_s << D$, *but* not for alluvial river beds.

The particle settling velocity V_s in still water given by [21] is

$$V_s = \frac{(s-1)gD^2}{C_1\nu + \left(0.75C_2(s-1)gD^3\right)^{0.5}} \qquad \text{[m/s]} \qquad [17]$$

where C_1 = 18, and C_2 = 1.0 for natural sediment.

2.2.5. *Invert properties*

The material strength can be expressed as a tensile or compression strength. In geomorphological research the bedrock abrasion is correlated to the

splitting tensile strength f_t [11], whereas in civil engineering research, the concrete abrasion is mostly related to the compression strength f_c [12, 22]. The parameter f_c has to be determined from a standard test procedure given for example in the Swiss Code SIA162/1.

The saltation-abrasion model in Eq. (1) implies the splitting tensile strength f_t. As the correlation between f_t and f_c is not constant [23], its use in the modified abrasion model in Eq. (2) is kept. Based on [23] f_t can be calculated from f_c in the following way:

$$f_t = 0.387 f_{c,cyl}^{0.63} \quad \text{[MPa]} \qquad [18]$$

The compression strength f_c can be obtained from two different test procedures. Samples are either cubed or cylindrical, and their correlation is given by

$$f_{c,cyl} = \beta f_{c,cube} \quad \text{[MPa]} \qquad [19]$$

where β = 0.8 = correlation coefficient according to Eurocode EN 1992-1-1. The Young's modulus Y_M should be simultaneously determined with f_c by means of laboratory load tests. However, if strain length data are not available the following equation can be used [24]

$$Y_M = k_1 k_2 \cdot 33500 \left(\frac{f_{c,cyl}}{60} \right)^{(1/3)} \left(\frac{\rho_c}{2400} \right)^2 \quad \text{[MPa]} \qquad [20]$$

where ρ_c = concrete density. The correction factors k_1 and k_2 account for the type of coarse aggregate and admixtures, respectively (Table 1 and 2). For other invert materials such as cast basalt plates or granite linings the material properties have to be determined assuming that the abrasion process of these non-cementitious inverts is similar to concrete.

Table 1
Practical values for correction factor k_1 in Eq. (20) [20], [24]

Lithological type of coarse aggregate	k_1
Crushed limestone, calcined bauxite	1.20
Crushed quartzite aggregate, crushed andesite, crushed basalt, crushed clayslate, crushed cobblestone	0.95
Coarse aggregate other than above	1.0

Table 2
Practical values for correction factor k_2 in Eq. (20) [20], [24]

Type of additive	k_2
Silica fume, ground-granulated blast-furnace slag, fly ash fume	0.95
Fly ash	1.10
Addition other than above	1.0

2.3. CALCULATION EXAMPLE

In the following a brief example to calculate the abrasion depth due to sediment transport is given using the case of the Solis SBT in Switzerland. This SBT is operated by the electric power company of Zurich, *ewz,* and was inaugurated in 2012. The tunnel connects the Solis reservoir with the Albula torrent downstream of the dam. Further details are described in [25].

The design of the intake differs from other prototype examples as it is located 450 m upstream of the dam and not at the reservoir head. The intake bottom is located below the minimum reservoir level. Thus the intake inflow is pressurized and not conveyed at free-surface flow conditions. An acceleration section is not required as the free surface open channel flow downstream of the Tainter gate is already supercritical due to the pressurized inflow providing sufficient energy head. The cross-sectional profile is of archway type. The tunnel invert slope downstream of the Tainter gate is constant with S_b = 0.019 and the invert is lined with a high performance concrete C70/85.

The Albula river parameters upstream of the reservoir are:

- HQ5 = 170 m^3/s
- B = 50 m (estimate)
- S_b = 0.01 (estimate)
- D_m = 6.0 cm
- D_{30} = 1.5 cm
- D_{90} = 15.0 cm
- n = 0.030 = $D_m^{1/6}$/21 (corresponding to $D_m \approx$ 6 cm)
- ρ_s = 2,650 kg/m^3
- θ_c = 0.05 (typical value for gravel bed rivers)

The tunnel dimensions and hydraulic parameters are:

- Q_d = HQ5 = 170 m^3/s
- L_t = 968 m
- b_t = 4.40 m
- S_b = 0.019
- k_s = 3 mm (assumption, slightly abraded concrete invert)
- θ_c = 0.002 (assumption for fixed bed based on [2])

The invert material parameters are:

- ρ_c = 2,400 kg/m^3 (estimate, standard value)
- f_c = 70×10^6 Pa (minimum requirement from the operator *ewz*)
- k_v = 10^6 (based on [12])

For the Albula river the following calculations are made for a 5-year flood:

- Eq. (7) leads to h = 1.01 m
- $R_h \approx B \cdot h/(B+2h)$ = 0.97 m (for rectangular cross-section)
- Eq. (6) leads to U = 3.29 m/s
- Eq. (5) leads to θ = 0.098
- Eq. (8) leads to q_{vn}^* = 0.042 [-], i.e. $q_v^* = q_{vn}^* \cdot ((s-1)g D_m^3)^{1/2}$ = 0.0025 m^3/(sm) and $Q_v^* = q_{vn}^* \cdot B$ = 0.124 m^3/s, or equally $Q_s^* = Q_v^* \cdot \rho_s$ = 329 kg/s

From the backwater curve calculation follows that the uniform (index u) flow depth in the tunnel of h_u = 3.64 m is reached 850 m downstream of the gate. For sake of simplicity the following example is calculated with the uniform flow values:

- Eq. (3) leads to $U_{co,u}$ = 10.6 m/s
- $R_{h,u} \approx b_t \cdot h_u/(b_t + 2h_u)$ = 1.37 m (for rectangular cross-section)
- Eq. (4) leads to U_* = 0.51 m/s
- Eq. (5) leads to θ = 0.263
- Eq. (10) leads to $Q_s^* = q_s^* \cdot b_t$ = 3,495 kg/s
- Eq. (11) leads to $Q_s^* = q_s^* \cdot b_t$ = 5,604 kg/s

- Eq. (12) leads to $Q_s^* = q_s^* \cdot b_t = 2{,}208$ kg/s (most conservative)
  → *Requirement:* $Q^*_{s,tunnel} = 2{,}208$ kg/s > $Q^*_{s,river} = 329$ kg/s fulfilled
- Eq. (14) leads to $W_{im} = 0.51$ m/s
- Eq. (17) leads to $V_s = 1.14$ m/s (with $D = D_m$)
- Eq. (16) leads to $I = 0.215$/m
- Eq. (18) leads to $f_t = 5.63 \times 10^6$ Pa
- Eq. (20) leads to $Y_M = 35{,}266 \times 10^6$ Pa

Finally, for the calculation of the abrasion depth, the sediment effectively supplied by the Albula river and flushed through the tunnel, i.e. $q_s = Q_s^*/b_t = 329$ kg/s/4.4 m = 74.7 kg/(sm) is inserted into Eq. (2) instead of the theoretical sediment transport capacity of the tunnel $q_s^* = 2{,}208/4.4 = 502$ kg/(sm). Thus the vertical abrasion rate from Eq. (2) follows as $A_r = 4.58 \cdot 10^{-9}$ m/s or as a gravimetric abrasion rate of $A_{rg} = A_r \cdot b_t \cdot \rho_c = 4.58 \cdot 10^{-9}$ m/s·4.4 m·2400 kg/m^3 = $4.84 \cdot 10^{-5}$ kg/s per meter tunnel length. Based on the tunnel length of 968 m, the total gravimetric vertical abrasion in the whole tunnel amounts to 0.047 kg/s. Assuming a typical spilling duration of 12 hours for a HQ5 flood leads to a vertical abrasion depth of $h_a = 0.2$ mm and a total mass loss of 2.02 tons.

3. FIELD RESEARCH STUDY

3.1. IN-SITU EXPERIMENT SITES

3.1.1. Runcahez sediment bypass tunnel

The Runcahez reservoir provides a storage capacity of 0.44 Mm^3 impounding the runoff of a 56 km^2 catchment area [26]. The facility including a SBT was built in 1962. The tunnel runs several days a year during flood periods.

In the 1990s, a test set-up consisting of a monitoring system and five different concrete mixtures was installed [27]. The abrasion rates were calculated based on yearly bed elevation measurements. Since the termination of this study, no further measurements of hydraulic operating conditions and abrasion have been conducted. The abrasion damages over the last 15 years were low and hence no refurbishment of the test fields was required. The advanced maturing invert test fields will be resurveyed in order to extend the former investigation and gain long time experiences.

3.1.2. Solis sediment bypass tunnel

The Solis reservoir, impounding a volume of 4.1 Mm^3, was commissioned 1986 [25]. The catchment comprises about 900 km^2 providing about 110,000 m^3 of sediments and causing mean reservoir aggradation of 80,000 m^3 on average per year. In order to avoid blockage of the outlet structures and to stop or at least reduce reservoir capacity loss due to sedimentation, a SBT was constructed [3, 25]. The facility diverts sediment-laden flood peaks returning statistically once a year or less.

Beside six test fields equipped with different invert materials (various high strength concretes, steel and cast basalt), a measurement system was implemented to continuously measure hydraulic operating conditions and monitor sediment transport [3]. The transport rates of suspended and bed-load sediments were estimated based on turbidity and geophone measurements, respectively. Thereby sieve analysis of the aggradation and estimated sediment transport capacity of the approach flow towards the intake are considered. Furthermore, regular laser scans have been conducted to determine abrasion rates and to analyze the correlation between impact, material properties and abrasion resistance.

3.1.3. Pfaffensprung

The Pfaffensprung reservoir was built in 1922, impounding the Reuss river, and draining a catchment of about 390 km^2 [3, 26]. With 0.17 Mm^3 the reservoir capacity is very small compared to the mean annual runoff of 645 Mm^3. Therefore the facility was equipped from the beginning with a sediment bypass tunnel, discharging large amounts of sediment and water during summer season, when discharge exceeds the threshold for sediment transport.

At this site four different test fields equipped with granite plates and high strength concretes are monitored. While the discharge is continuously measured, no measurement device is available to quantify sediment transport rates. The invert mass loss is determined based on laser scans taken every year.

3.2. FIELD RESULTS

3.2.1. Runcahez

Since the measurements at this site will be carried out in Winter 2014/2015 they are not part of this article. However, the results gained in the former project show reliable tendencies [22].

From the beginning, the bed abrasion was concentrated at the inner tunnel section downstream of a bend. Secondary flow patterns induced by curvatures

caused sediment transport concentration in this section leading to higher invert impact and thus higher abrasion. The abrasion generally exhibited an adulating pattern, with material loss concentrations at vulnerabilities and discontinuities. Thus the implementation procedure strongly influences the homogeneity of the morphology, the cohesion between cement matrix and aggregates and thus the durability of the concrete. This effect is strongly visible at a roller compacted concrete field. The areas near the walls could not be compacted sufficiently and thus suffer material losses more than one order of magnitude higher compared to the rest.

Material loss is disclosed to depend on bending tensile strength and fracture energy reciprocally, while the material loss and the compression strength did not exhibit a clear correlation. Nevertheless, the mass loss produced by laboratory abrasion tests after [27] and the abrasion rates in the field depended linearly to each other.

3.2.2. Solis

Since the commissioning, the Solis SBT was operated four times. The bypassed discharged varied around 85 m^3/s, which is slightly under Q_{min} = 90 m^3/s, and 170 m^3/s, corresponding to design discharge, Q_d. The return period of the flood peak was generally less than one year corresponding to the minimal operation discharge. However, in August 2014 the SBT was in operation during a greater than 10 year flood event. The average operation duration was about 11 hours.

Due to changes of the aggradation body in the reservoir during the construction phase, the bedload transport rate was much lower than the transport capacity and expected rate and thus no significant abrasion was observed during the first three operations. The first event provoking slight abrasion marks was in August 2014. Although laser scan of the tunnel invert will be made in the following winter season, visual assessment showed that the upstream edges of the cast basalt plates were abraded and recognizable by the light gray color as shown in Fig. 3.

In Solis SBT, there is a curvature downstream of the test fields. The bedload transport measurements using geophone system installed 100 m downstream of the bend, still showed a sediment transport concentration at the inner side of the curvature, confirming the observations gained at Runcahez.

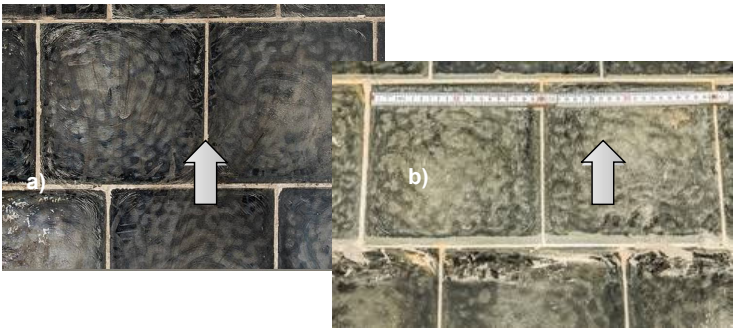

Fig. 3
Picture (45 cm x 30 cm) of cast basalt plates (a) after implementation and before first operation and (b) two years after commissioning.
Photo (45 cm x 30 cm) de carreaux basaltiques (a) après la mise en œuvre et avant la mise en service et (b) deux ans après la mise en service.

3.2.3. Pfaffensprung

The Pfaffensprung SBT features also a bend after the intake and similar to the above mentioned tunnels, abrasion marks indicted that bed load transport was concentrated on the inner side of the tunnel and propagated downstream. The mean abrasion depth of the implemented high strength concretes was about 1.4 cm per year, which is five times higher than that of the granite plate linings. While the abrasion pattern of the concrete was wavy and evenly distributed (except for the curvature effect), the abrasion on the granite plates was concentrated at the joints. Outstanding edges adjusted against the flow direction were observed to suffer the highest abrasion.

4. DESIGN RECOMMENDATIONS

General design recommendations for SBTs yield from the findings gained by the laboratory model study and in-situ experiments are summarized below.

The specific particle impact energy on the invert scales quadratically with the impact velocity. A linear relationship between the particle impact velocity and the streamwise flow velocity was found in the laboratory study [2]. The crucial parameter primarily affecting the invert abrasion is the flow velocity. In turn, the flow velocity in an open channel flow is controlled by the invert width and the in-

vert slope for a given design discharge. Reducing the slope or increasing the width reduces the flow velocity. However, the velocity has to be higher than the critical velocity above which no sediment deposition occurs. As the research on sediment transport on fixed and smooth or transitionally rough beds is scarce, the formulae by [2, 16, 17] should be used and compared to estimate the transport capacity and critical velocity in the tunnel. These values have to exceed the bed-load transport capacity calculated in the upstream river section by means of state of the art formulae for movable river beds [13, 20] to secure a safe bypassing of the sediments without accumulation in the tunnel.

The question arises whether the bed slope or invert width additionally affect the impact energy and invert abrasion development other than increasing the streamwise flow velocity. It was found in the laboratory study that varying the bed slope does not additionally affect the abrasion in the studied range. The saltation length as another parameter directly affecting the impact energy linearly scales with the flow velocity, but does not reveal additional effects of bed slope. In other words, a steep bed slope only contributes to a higher flow velocity, but other than that does neither additionally affect the particle trajectory and consequently nor the impact energy and invert abrasion. Also, the direct abrasion measurements in phase C of the research project do not reveal exceptionally high abrasion rates for the steep slope experiments.

In contrast to the bed slope, variation of the invert width does change the abrasion development by affecting the secondary current flow pattern and as a consequence changing the bed shear stress distribution. For narrow open channel flows with $b/h < 3\text{-}4$ steep lateral sidewall incision channels develop, whereas for higher ratios $b/h > 3\text{-}4$ these channels decrease in their extent and additionally randomly distributed potholes develop.

To conclude, a relatively large tunnel width should be considered to achieve a more even bed shear stress distribution, where resulting abrasion is more evenly distributed. Otherwise, for low aspect ratios, steep incision channels develop, and provoke a self-intensifying effect and hence more sediment is transported in these channels. If narrow open channel flow cannot be avoided, an invert strengthening at both sides of the tunnel along the walls should be considered.

Curves in plan-view should be avoided or at least constructed with a preferably large radius as sediment transport always occurs on the inner side of the curve due to the development of additional secondary currents. Similar to the area in the side wall vicinity at straight sections, an invert strengthening along the inner curve should be considered to cope with the increased specific sediment transport rates.

Finally, invert irregularities and vulnerabilities at joints or imprecise uneven invert implementation should be avoided or at least minimized. The experiments

clearly reveal that excessive irregularities directly cause initiation of abrasion. Additional recommendations are published in [28].

5. CONCLUSIONS

5.1. LABORATORY RESEARCH STUDY

A modified formula to estimate the abrasion rate on tunnel inverts at supercritical flows is introduced in [12] using results of [2, 10] based on the *saltation abrasion model* by Sklar and Dietrich [11]. The gravimetric abrasion rate depends on (1) the acting forces described by the impact energy, saltation trajectory and saltation and suspension probabilities, and (2) the invert material resistance described by the material strength, Young's modulus, and material density. The abrasion coefficient k_v correlate (1) and (2) with the abrasion rate. In [12] the derivation of the abrasion coefficient is explained in detail and its value can be approximated with $k_v = 10^6$.

5.2. FIELD RESEARCH STUDY

The abrasion resistance of different concretes, natural stone material and steel has been investigated by conducting in-situ experiments at three sediment bypass tunnels located in the Swiss Alps. The materials exhibit characteristic abrasion patterns and are influenced by irregularities and vulnerabilities on the invert. Beside the material properties the invert implementation procedure plays a significant role concerning invert durability and abrasion resistance.

Beside determination of the most abrasion resistant and economic material considering site-specific conditions, field measurement enable calibration of the abrasion model developed based on the laboratory experiments. As a result the formula presented here (Eq. (2)) will be used to predict the abrasion depth and hence service life time for field applications.

ACKNOWLEDGEMENTS

The first author kindly acknowledges the support of the *Japanese Society for the Promotion of Science*. Furthermore, the authors would like to thank swiss*electric* research, the Swiss Federal Office of Energy (SFOE), *CemSuisse*,

Fondazione Lombardi, the electric power company of Zurich (ewz) and the Swiss Federal Railways (SBB) for their supports.

REFERENCES

[1] AUEL C., BOES R.M. Sustainable reservoir management using sediment bypass tunnels. *Proc. 24th ICOLD Congress*, Kyoto, Japan, Q92, R16, 224–241, 2012.

[2] AUEL C. Flow characteristics, particle motion and invert abrasion in sediment bypass tunnels. *PhD Thesis* 22008, also published as *VAW-Mitteilung 229* (R.M. Boes, ed.), ETH Zurich, Switzerland, 2014.

[3] HAGMANN M., ALBAYRAK I., BOES R.M. Reduktion der Hydroabrasion bei Sedimentumleitstollen - In-situ-Versuche zur Optimierung der Abrasionsresistenz ('Reduction of hydroabrasion in sediment bypass tunnels – In-situ experiments to optimize the abrasion resistance'). *Proc. Inter. Wasserbausymposium*, (G. Zenz, ed.), TU Graz, Austria, 91–97, 2012 [in German].

[4] HAGMANN M., ALBAYRAK I., BOES R.M. Untersuchung verschleissfester Materialien im Wasserbau mit einer Geschiebetransportüberwachung ('Study on abrasion-resistant materials in hydraulics with a sediment transport monitoring'). *Proc. Intl. Symposium "Wasser- und Flussbau im Alpenraum", VAW-Mitteilung 227* (R.M. Boed, ed.), ETH Zurich, Switzerland, 97–106, 2014 [in German].

[5] SCHWALT M., HAGER W.H. Die Strahlbox ('The jet box'). *Schweizer Ingenieur und Architekt*, 110(27-28), 1992 [in German].

[6] FINNEGAN N.J., SKLAR L.S., FULLER T.K. Interplay of sediment supply, river incision, and channel morphology revealed by the transient evolution of an experimental bedrock channel. *J. Geophysical Res.: Earth Surface* 112(F3), 2007.

[7] JOHNSON J.P., WHIPPLE K.X. Feedbacks between erosion and sediment transport in experimental bedrock channels. *Earth Surface Processes And Landforms* 32(7): 1048-1062, 2007.

[8] JOHNSON J.P., WHIPPLE K.X. Evaluating the controls of shear stress, sediment supply, alluvial cover, and channel morphology on experimental bedrock incision rate. *J. Geophysical Res.: Earth Surface* 115, 2010.

[9] AUEL C., ALBAYRAK I., BOES R.M. Turbulence characteristics in supercritical open channel flows: Effects of Froude number and aspect ratio. *J. Hydraulic Eng.* 140(4), 04014004, 16 pages, 2014.

[10] AUEL C., ALBAYRAK I., BOES R.M. Particle motion in supercritical open channel flows. *J. Geophysical Res.: Earth Surface*, in preparation, 2015.

[11] SKLAR L.S., DIETRICH W.E., A mechanistic model for river incision into bedrock by saltating bed load. *Water Resources Research* 40(6), 2004.

[12] AUEL C., ALBAYRAK I., SUMI T., BOES R.M. Saltation-abrasion model for hydraulic structures. *Proc. 1st Int. Workshop on Sediment Bypass Tunnels*, Zurich, Switzerland, 2015.

[13] WONG M., PARKER G. Reanalysis and correction of bed-load relation of Meyer-Peter and Müller using their own database. *J. Hydraulic Eng.* 132(1), 1159–1168, 2006.

[14] MEYER-PETER E., MÜLLER R. Formulas for bedload transport. *Proc. 2nd Meeting Int. Association of Hydraulic Structures Research*, Stockholm, Sweden, 39–64, 1948.

[15] BUFFINGTON J.M., MONTGOMERY D.R. A systematic analysis of eight decades of incipient motion studies, with special reference to gravel-bedded rivers. *Water Resources Research* 33(8), 1993–2029, 1997.

[16] PEDROLI R. Trasporto di material solido in canali a fondo fisso e liscio (Transport of solid material in channels on a fixed and smooth bed). *Mitteilung des Eidg. Amtes für Wasserwirtschaft 43*, Eidgenössisches Verkehrs- und Energiewirtschaftsdepartement, Switzerland, 1963 [in Italian].

[17] SMART G.M, JÄGGI M.N.R. Sediment transport on steep slopes. *VAW-Mitteilung 64* (D. Vischer, ed.), ETH Zurich, Switzerland, 1983.

[18] CHATANANTAVET P., WHIPPLE K.X., ADAMS M.A., LAMB M.P. Experimental study on coarse grain saltation dynamics in bedrock channels. *J. Geophysical Res.: Earth Surface* 118(2), 1161–1176, 2013.

[19] HU C., HUI Y. Bed-load transport. I: Mechanical characteristics. *J. Hydraulic Eng.* 122(5), 245–254, 1996.

[20] FERNANDEZ LUQUE R., VAN BEEK, R. Erosion and transport of bedload sediment. *Journal of Hydraulic Research* 14(2), 127–144, 1976.

[21] FERGUSON R.I., CHURCH M. A simple universal equation for grain settling velocity. *J. Sedimentary Res.* 74(6), 933–937, 2004.

[22] JACOBS F., WINKELER W., HINKELER F., VOLKART P. Betonabrasion im Wasserbau: Grundlagen, Feldversuche, Empfehlungen ('Concrete abrasion at hydraulic structures: Fundamentals, field experiments, recommendations'). *VAW-Mitteilung 168* (H.-E. Minor, ed.), ETH Zurich, Switzerland, 2001 [in German].

[23] ARIOGLU N., CANAN GIRIN Z., ARIOGLU E. Evaluation of ratio between splitting tensile strength and compressive strength for concretes up to 120 MPa and its application in strength criterion. *ACI Materials Journal* 103(1), 18–24, 2006.

[24] NOGUCHI T., TOMOSAWA F., NEMATI K.M., CHIAIA B.M., FANTILLI, A.P. A practical equation for elastic modulus of concrete. *ACI Structural Journal* 106(5), 690–696, 2009.

[25] AUEL C., BOES R., ZIEGLER T., OERTLI C. Design and construction of the sediment bypass tunnel at Solis. *Hydropower and Dams* 18(3), 62–66, 2011.

[26] VISCHER D., HAGER W. H., CASANOVA C., JOOS B., LIER P., MARTINI O. Bypass tunnels to prevent reservoir sedimentation. *Proc. 19th ICOLD Congress*, Florence, Italy, 605-624, 1997.

[27] BANIA A. Bestimmung des Abriebs und der Erosion von Beton mittels eines Gesteinsstoff-Wassergemisches (Determination of abrasion and

erosion of concrete by means of a sediment-water mixture). *Doctoral Thesis*, Wismar, Germany, 1989 [in German].

[28] BOES R.M., AUEL C., HAGMANN M., ALBAYRAK I. Sediment bypass tunnels to mitigate reservoir sedimentation and restore sediment continuity. *Reservoir Sedimentation* (A.J. Schleiss, G. De Cesare, M.J. Franca, M. Pfister, eds.), ISBN 978-1-138-02675-9, Taylor & Francis Group, London, UK: 221-228, 2014.

SUMMARY

In order to prevent reservoir sedimentation, sediment bypass tunnels can be an efficient countermeasure restoring sediment continuity of impounded rivers. Although supercritical open channel flow conditions in these tunnels prevent tunnel blockage, in combination with the high bypassed sediment volume it may lead to severe abrasion damages on inverts. Consequently, wear termed hydroabrasion occurs. Based on laboratory experiments, a theoretical model was developed to predict abrasion rates and service life time of sediment bypass tunnels. *In-situ* experiments are further conducted for model calibration to provide an abrasion prediction approach for field applications. Finally, recommendations concerning the hydraulic design of the tunnel as well as the structural design of the invert are provided.

RÉSUMÉ

Pour combattre l'alluvionnement des réservoirs, les galeries de dérivation de sédiments constituent une mesure efficace, permettant même une continuité d'écoulement des sédiments dans la rivière retenue. Les écoulements torrentiels évitent le bouchage de la galerie, mais en raison du grand volume de sédiments emportés, ils ont un impact important sur le radier. Une usure nommée hydroabrasion apparaît alors. Pour prévoir les taux d'abrasion et la durée de vie, une formule se basant sur des expérimentations en laboratoire a été développée. Des essais *in situ* ont été menés par ailleurs pour étalonner le modèle analytique pour une application pratique. Pour finir, des recommandations, concernant à la fois la conception hydraulique du tunnel et la conception de la structure du radier sont fournies.